Manipulating Protein Conformations by Single-Molecule AFM-FRET Nanoscopy

Yufan He, Maolin Lu, Jin Cao, and H. Peter Lu*

Center for Photochemical Sciences, Department of Chemistry, Bowling Green State University, Bowling Green, Ohio 43403, United States

ABSTRACT

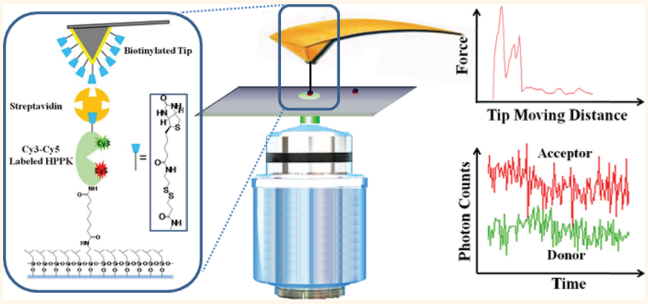

Combining atomic force microscopy and fluorescence resonance energy transfer spectroscopy (AFM-FRET), we have developed a single-molecule AFM-FRET nanoscopy approach capable of effectively pinpointing and mechanically manipulating a targeted dye-labeled single protein in a large sampling area and simultaneously monitoring the conformational changes of the targeted protein by recording single-molecule FRET time trajectories. We have further demonstrated an application of using this nanoscopy on manipulation of single-molecule protein conformation and simultaneous single-molecule FRET measurement of a Cy3–Cy5-labeled kinase enzyme, HPPK (6-hydroxymethyl-7,8-dihydropterin pyrophosphokinase). By analyzing time-resolved FRET trajectories and correlated AFM force pulling curves of the targeted single-molecule enzyme, we are able to observe the protein conformational changes of a specific coordination by AFM mechanic force pulling.

KEYWORDS: single-molecule AFM-FRET nanoscopy · enzyme · force pulling manipulation · conformational changes

Protein conformations play crucial roles in protein functions.[1–5] The new paradigm of the protein structure–function relationship is that the dynamics of protein structural fluctuations play critical roles in protein functions.[6–9] For example, protein functions in enzymatic catalysis and protein–protein interactions involve protein conformational fluctuations and folding–binding cooperative interactions.[10–13] An enzyme can have different activities with different conformations,[14–16] and conformational changes can significantly change the affinity and selectivity of protein interactions, which in turn often contribute to dramatic changes in protein functions.[17–19] Thus, manipulating protein conformations can be effective for changing, enhancing, or even creating protein functions. It has been theoretically suggested that an oscillating force applied to an enzyme at a comparable frequency of enzymatic reaction turnover rate changes the enzymatic reaction activities due to force modification of the reaction pathway, potential surface, and enzymatic reaction intermediate state energy.[20,21] In recent years, experimental works have demonstrated that external mechanical force can change protein activities;[22,23] accordingly, real-time measurements of protein conformational dynamics with a combined external force to manipulate and even control protein structures are a promising approach for protein structure–function studies.

Single-molecule approaches are proved to be powerful and informative in characterizing protein functions, conformations, and activities, which are beyond the conventional ensemble-averaged measurements.[24–26] In another respect, AFM and correlated single-molecule force spectroscopy has been proved to be specified for studying protein conformations and activities under physiological conditions.[27,28] Thus, a combination of correlated single-molecule spectroscopy with atomic force microscopy is ideal for obtaining the identified structural information or direct observation of the effect of external mechanical perturbation on the protein and related enzymatic activity in real time. Progress has been achieved in combining single-molecule spectroscopy measurements and simultaneous AFM manipulations.[29–33] For example, Fernandez and co-workers introduced a combined AFM-TIRF microscopy and used a fluorescence-labeled cantilever to pull and unfold tethered polyubiquitin between the sample surface and cantilever tip.[30] This combination provides a method to monitor a fluorescently labeled molecule

* Address correspondence to hplu@bgsu.edu.

Received for review October 7, 2011 and accepted January 25, 2012.

Published online January 25, 2012
10.1021/nn2038669

moving vertically along the *z*-axis and potentially can be used to track the activity of single molecules simultaneously. Gaub and co-workers also used an integrated AFM-TIRF to read out the influence on the enzymatic activity by AFM-induced periodic stretching and relaxation of enzymatic conformation through simultaneous fluorescence imaging, and they reported that relaxation from the force-induced enzyme conformation led to higher catalytic activity after the external stretching force on the enzymes was released.[29] The advantage of the integrated AFM-TIRF microscopy is that collecting optical signals is relatively easy due to the large imaging area of TIRF. However, there also exists an apparent disadvantage in the correlated single-molecule force manipulation and fluorescence total reflection imaging microscopy measurements, which is that the signals from optical measurement may not come from the target molecule that is manipulated by AFM. For example, in this AFM-TIRF study of the influence on the enzymatic activity by AFM-induced periodic stretching and relaxation of enzymatic conformation through simultaneous fluorescence imaging experiment, the enzyme molecules themselves cannot be directly labeled for probing the conformational changes or monitoring enzymatic reaction motions under high enzyme concentration within the imaging sample area; only the fluorogenic product molecules can be measured. Therefore, many of the time-resolved and polarization-resolved single-molecule spectroscopy measurements cannot be applied. Furthermore, the measured enzymatic reaction product is probably not the specific one from the exact target enzyme molecule perturbed by the AFM tip.

Kodama and co-workers have made an advancement in using a confocal laser scanning microscope correlated with AFM to probe the relationship between protein structure and function by observing the fluorescence change of green fluorescent protein when a compression or extension force is applied to the protein.[31] However, this measurement is not at the single-molecule level; about 30 protein molecules under the microbead are attached to the ATM tip. In fact, there is an apparent conflict of preference and intrinsic technical dilemma between the high concentration requirement of sample molecules for AFM manipulation and low concentration requirement for single-molecule optical spectroscopy. Single-molecule spectroscopy requires that the fluorescent probe molecules are distributed at a low concentration of 10^{-9} to 10^{-10} M or on average one target molecule per μm^2 area. In contrast, conventional AFM force pulling experiments require a high concentration, near monolayer, of proteins on the sampling surface, as an AFM tip cannot specifically pinpoint a targeted protein molecule in a sample area larger than 1 μm^2.

There are rich technical approaches of single-molecule spectroscopy, including confocal imaging, TIRF, single-molecule FRET, tip-enhanced near-field spectroscopy and imaging, *etc.*,[29−33] that have been combined with the AFM-correlated microscopy, but to our knowledge, there are no such approaches that have reached single-molecule level. There is a simple and critical reason that the technical bottleneck that has been prohibiting various above-mentioned single-molecule microscopy and spectroscopy approaches from being combined with the AFM force manipulation analysis. The reason is that for these types of single-molecule spectroscopic approaches to be applied, the single-molecule protein has to be fluorescent by intrinsic fluorescence or by dye-probe labeling, and the fluorescence molecule can only be a single one distributed in a 10^{-10} M concentration within a large sample area, that is, about one molecule in each μm^2. The reality of such a diluted sample requires that the AFM tip is capable of pinpointing the individual molecule in a sample area that is much larger than a typical AFM single-molecule imaging sampling area. Nevertheless, a direct correlation between measuring single-molecule activity and specifically manipulating conformational changes has not been achieved yet. In this article, we report our new technical approach of an AFM-FRET nanoscopy capable of simultaneous measurements of single-molecule force spectroscopy and FRET spectroscopy for a targeted single protein molecule. By recording and analyzing single-molecule FRET time trajectories of a Cy3−Cy5-labeled kinase protein and correlated force spectroscopy on the same molecule, we have demonstrated the experimental approach of simultaneous single-molecule spectroscopic measurements of protein conformational changes under AFM tip manipulations. Our AFM-FRET nanoscopy approach enables us to study the relation between protein structure and function at a pinpointed single-molecule level.

In our experiments, HPPK (6-hydroxymethyl-7,8-dihydropterin pyrophosphokinase), a 35 kDa 158-residue monomer kinase enzyme protein,[34,35] was studied. HPPK catalyzes the pyrophosphorylation reaction that leads the conversion of 6-hydroxymethyl-7,8-dihydropterin (HP) to 6-hydroxymethyl-7,8-dihydropterin pyrophosphate (HPPP) in the presence of ATP during the folate biosynthesis pathway in bacterial cells. There are three flexible loops of HPPK involved in the enzymatic catalysis reaction (Figure 1).[5,34] Among them, loop 3 undergoes dramatic open−close conformational changes in each catalytic cycle, correlating with substrate (ATP and HP) binding. To probe the single-molecule conformational change of protein under the AFM force pulling perturbation, the enzyme HPPK was labeled with Cy3/Cy5 on the amino acid residue 88 on loop 3 and residue 142 on the protein core close to the enzymatic active site of the enzyme,[35] respectively (Figure 1A). To apply mechanical force to perturb the conformation of a single enzyme molecule using the

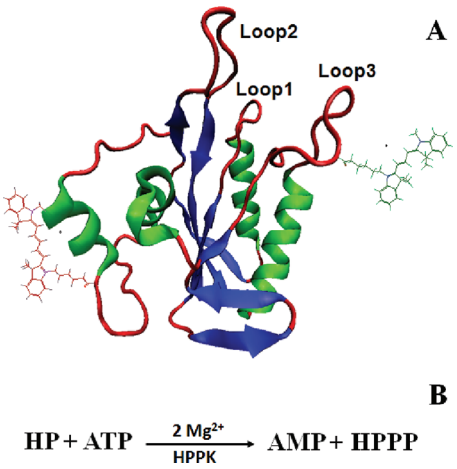

Figure 1. (A) Crystal structure of HPPK. The green spirals represent α helices and the blue arrows represent β strands. The loops are shown by the red pipes. Amino acid residues 88 and 142 have been labeled with FRET dye pair Cy3 and Cy5, respectively. (B) HPPK-catalyzed pyrophosphorylation transfers two phosphor groups from ATP to HP.

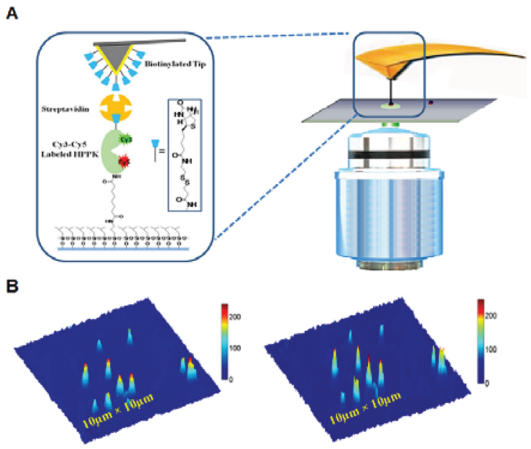

Figure 2. (A) Single-molecule AFM-FRET ultra-nanoscopy. The zoomed-in panel on the left presents a schematic diagram of one FRET dye pair (donor–acceptor: Cy3–Cy5) labeled HPPK molecule tethered between a glass coverslip surface and a handle (biotin group plus streptavidin), and another biotin group is modified on the AFM tip. (B) Single-molecule fluorescence photon counting images of the donor (Cy3, left) and acceptor (Cy5, right). Each feature is from a single HPPK enzyme labeled with Cy3–Cy5 FRET dyes.

AFM tip, we coupled HPPK molecules between a glass coverslip and a "handle" function group (biotin and streptavidin) for the AFM tip through amine groups on the protein (Figure 2A).

RESULTS AND DISCUSSION

In our single-molecule AFM-FRET nanoscopy, time-resolved FRET trajectories and correlated AFM force pulling curves of the targeted single HPPK enzyme are simultaneously recorded during the whole pulling approach–retract cycle. Figure 3 presents the typical data recorded from an effective AFM pulling event, showing the FRET donor–acceptor intensity trajectories (Figure 3A, B), the correlated FRET efficiency trajectory (Figure 3C), and the correlated AFM force curve (Figure 3D). In a single AFM tip approach–retract cycle, the AFM tip travels about 600 nm down and 600 nm up; the total route is about 1200 nm within 2 s. There is a period about 0.5 s when the fluorescence intensity is three times higher than the flat area in the trajectory. Thus, the total traveling distance of back and forth in the field that enhanced fluorescence intensity is 300 nm, so the distance between the AFM tip and sample is estimated as 0 to 150 nm. The enhancement of the fluorescence intensity is due to a micromirror effect; that is, the AFM tip serves as a mirror reflecting the optical signal down to the microscopic objective, resulting in a higher single collection efficiency. The micromirror effect increases or decreases when the AFM tip gets close to or moves away from the laser focus spot on the sample surface in a correlated confocal single-molecule spectroscopic imaging measurement. The micromirror effect disappears when the tip is retracted back from the surface beyond the 150 nm range.

Figure 3A–C present the detection of FRET intensity, efficiency changes, and simultaneous AFM force spectrum when a pinpoint specific force pulling event occurs (Figure 3D). The changes of FRET efficiency (E_{FRET}) reflect the changes of the donor–acceptor distance associated with the protein unfolding by AFM force pulling.[36,37] Figure 3C shows a typical E_{FRET} time trajectory of single-molecule HPPK under AFM tip perturbation in the whole process of the AFM tip traveling route of approaching the protein from far away and then moving away out of the micromirror effect distance range. To distinguish a productive force pulling event from a nonproductive pulling event involving essentially similar AFM tip approaching–withdrawing movements, we analyzed the error bar of standard deviation on the correlated E_{FRET} signal measured under the tip approaching–withdrawing movements that occurred around a productive pulling event. The mean of the E_{FRET} when the tip is far from the surface (no mirror effect) is marked as first level. Similarly, the mean of the E_{FRET} when the tip is close to the surface (with a mirror effect) is marked second level (Figure 3C). It is statistically identifiable that the E_{FRET} signal, marked as the third level, correlated with a productive force pulling event. Therefore, as the tip approaches the single protein but not close enough to reach the micromirror effective distance (~150 nm), and as it moves far away beyond the 150 nm range, the E_{FRET} presents the first level, which is the normal level, without perturbation of the micromirror effect. As the tip reaches the range of the micromirror effect, E_{FRET} shifts to the second level. In this measurement, there are two factors that may affect the E_{FRET}: First is the mirror effect (both donor and acceptor fluorescence intensities increase when the tip reflects the optical signal down to the microscopic objective). In this case,

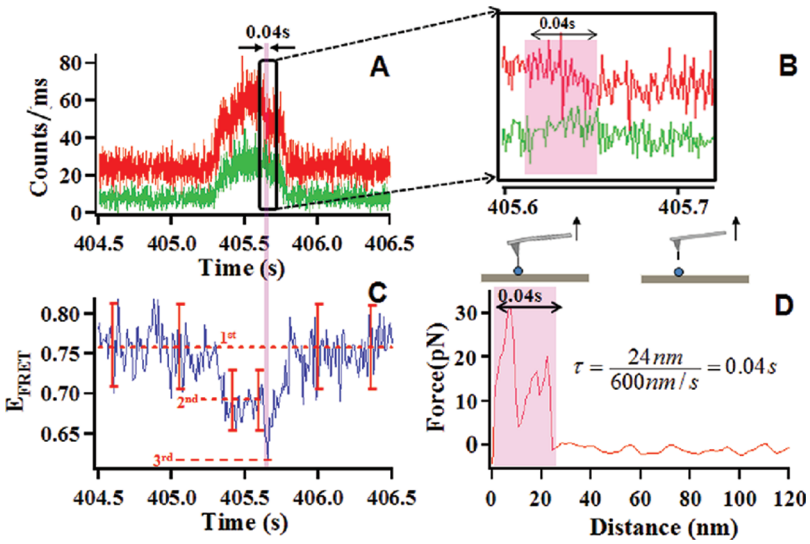

Figure 3. (A) Typical FRET time trajectory of donor (green) and acceptor (red) associated with one single-molecule AFM-FRET force pulling event. (B) Zoom-in intensity trajectory of donor and acceptor from (A); the highlighted intensity change is correlated to one pulling event occurring in 0.04 s. (C) FRET efficiency time trajectory of one single-molecule AFM-FRET pulling event, in the whole process of the AFM tip traveling route from approaching the protein from far away to moving away out of the micromirror effect distance range; three efficiency levels are recorded and identified. The error bar shows the ±2SD (standard deviation) indicating ≥95% precision of identification of the data points within the range. (D) Correlated force curve; the curve shows the extension length of 24 nm within a period of 0.04 s.

the increased efficiency may not be identical along the whole wavelength range, leading to different extents of efficiency changes in both channels. The second factor is plasma (plasma is generated from the Au-coated AFM tip excited by a laser). In this case, the intensity of the plasma is also probably not uniform in different wavelengths; that is, it may have different intensities in a different wavelength range. The third level E_{FRET} lasts only 0.04 s, which corresponds to the rapid extension process in which the protein is stretched by the AFM tip until the connection between the AFM tip and the protein ruptures. In the third level, 0.04 s period, E_{FRET} suddenly switches from the second level to the third one and then switches back; those changes reflect the protein conformational changes pulled by the AFM tip. Figure 3D shows the force curve from the simultaneous AFM measurement that is correlated to the FRET trajectory (Figure 3A, B, and C). The AFM force pulling curve (Figure 3D) shows two peaks and a total extension length of 24 nm. In this typical force curve, the extension length of 24 nm takes about 0.04 s to run across, which corresponds to the 0.04 s extension period in the corresponding FRET trajectory (highlighted in Figure 3A, B, and C).

The combination of force spectrum and correlated FRET recording enables us to identify the exact pulling site on a single HPPK molecule. Figure 4A, the statistical result of rupture distance, shows the primary distribution within a range of 20−40 nm and the mean extension length of about 24−28 nm. In this experiment, the amine groups on lysine residues were used to link the protein molecule to the coverslip surface and to the biotin handle for AFM tip manipulation. For the Cy3−Cy5-labeled (88c,142c) HPPK molecule, there are still five lysine residues (23, 85, 119, 154, 157) available. Therefore, there are a number of configurations associated with different linking residues for the single-molecule force pulling measurements, although there are only four possible unfolded configurations (between residue 23 and 85, between residue 85 and 154, between residue 85 and 157, or between residue 23 and 119 (see the Supporting Information, S1 for details), which gives the possible extension length ranging from 20 to 40 nm (Figure 4A). Among these possible unfolded configurations, the most possible linker is at residue 85. According to the literature, residue 85 is on loop 3, one of the important catalytic flexible loops of HPPK, correlating with substrate ATP binding, and undergoes the most dramatic open−close conformational changes in each catalytic cycle. Therefore, the force perturbation at residue 85 on loop 3 provides a most likely possibility of perturbing the enzyme−substrate binding and accordingly perturbing the enzymatic catalysis activity. Figure 4B, the histogram of the protein rupture force distribution, shows two peaks, 16−18 and 50−52 pN; the most possible rupture forces are in the range 16−18 pN. Our result is essentially consistent with the reported 10−60 pN rupture force values in single-molecule protein pulling, which is typically much smaller than the result of about a few hundreds pN in the rupture force measured in polymer force pulling experiments.[39,40] We suggest that, in our single-molecule force pulling experiment, the rupture force is due to an unfolding single loop, segment, or single domain that contains one or several hydrogen-bonding and other noncovalent chemical interactions.[38]

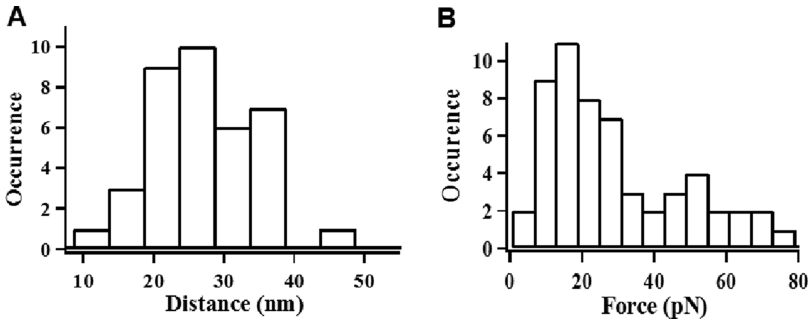

Figure 4. (A) Histogram of extension length distribution of AFM-FRET force unfolding single-molecule proteins. The primary extension length is within a range of 20−40 nm, and the mean extension length is about 24−28 nm. (B) Histogram of protein rupture force distribution. The distribution shows two peaks, and the most probable rupture forces are 16−18 and 50−52 pN.

However, the rupture force in protein polymer protein pulling[39,40] is the force of unfolding a whole protein within a protein polymer; that is, the rupture force includes not only the force of rupturing the multiple hydrogen bonds in a protein but also the force of rupturing all the associated hydrophobic forces and related chemical bonds that hold the whole protein in its folded state. Furthermore, the single enzyme domain rupture forces observed in our experiments are in a scale comparable with other reported single-molecule protein domain rupture forces.[28,41]

To further prove our attribution of the possible unfolded configurations between lysine residues in our single-molecule pulling experiment, we did a control experiment of the HPPK mutant (142C, Figure 5E). On one end of the linking, we chemically tether the HPPK molecule to the glass coverslip surface at a specific amino acid residue position (142) by mutation (see Supporting Information, S2 for details). For the other end, in order to be linked by chemical reaction to EZ-linker (NHS-SS-Biotin), the $-NH_2$ group on the HPPK amino acid side chains must be from one of the lysine residues except site 142, namely, sites 23, 85, 119, 154, and 157. However, the configurations between 142 and 154 or 157 are too close to be the origins of the measured force pulling curves, so there are actually only three possible unfolded configurations, and they are between amine acid residue 142 and amine acid residues 23, 85, and 119, respectively. Assuming the average distance is 3.8 Å in each amine acid residue, the overall distances of the force pulling curves are about 45.2, 21.7, and 8.7 nm, respectively.

The experimental results (Figure 5), obtained in tris-buffer plus $MgCl_2$ with the presence of enzyme prohibitor (AMPCPP, α,β-methyleneadenosine 5′-triphosphate), show three typical force curves. These force curves consist of sawtooth-shaped peaks. These peaks are the results of unfolding single HPPK molecules. The distances to rupture the protein from the force curves are 9 ± 2, 22 ± 3, and 46 ± 7 nm, respectively (Figure 5D). These results correspond to the possible unfolded configurations correlated to the protein domains between amino acid residue 142 and amino acid residues 119, 85, and 23, respectively. In addition, these experimental results (9 ± 2, 22 ± 3, and 46 ± 7 nm) are consistent with the theoretical results (8.7, 21.7, and 45.2 nm above). On the basis of the above results, we propose that three domains exist between residue 23 and residue 142, namely, DomA (green in Figure 5), DomB (purple in Figure 5), and DomC (red in Figure 5). Since there are only three unfolded configurations as discussed above, we investigate them separately (Figure 5A−C) and integrate the results into one probability distribution of rupture distances (Figure 5D). In the first configuration (119,142), as shown in Figure 5A, one end of HPPK is tethered to the glass coverslip through residue 142 when the other end is linked to the AFM tip via residue 119. In our model, DomC is unfolded by AFM tip pulling, and the experimental rupture distance is about 9 nm, which not only is consistent with the theoretical value of 8.7 nm but also completely agrees with the first peak (9 nm) of the rupture distance distribution (Figure 5D). In the second configuration (85,142), the pulling and tethering sites on HPPK are residue 85 and residue 142, respectively. As shown in Figure 5B, DomB and DomC are unfolded with a rupture distance around 22 nm; this experimental result is also consistent with the theoretical value of 21.7 nm and the second peak (22 nm) of the rupture distance distribution (Figure 5D). In the third configuration (23,142), as shown in Figure 5C, three proposed domains (DomA, DomB, and DomC) between site 23 and site 142 are all unfolded and thus give a larger rupture distance compared to only unfolding DomC (Figure 5A) or unfolding DomB and DomC (Figure 5B). Furthermore, the experimental value (45 nm), the expected theoretical value (45.2 nm), and the third peak (45 nm) in the distribution of rupture distances are all almost identical with each other. Therefore, in Figure 5, all three force curves fit well in our proposed three-domain model. Moreover, the rupture distance consistency of different domains among experimental values, theoretical values, and the distribution peaks reinforces our proposed three-domain explanation.

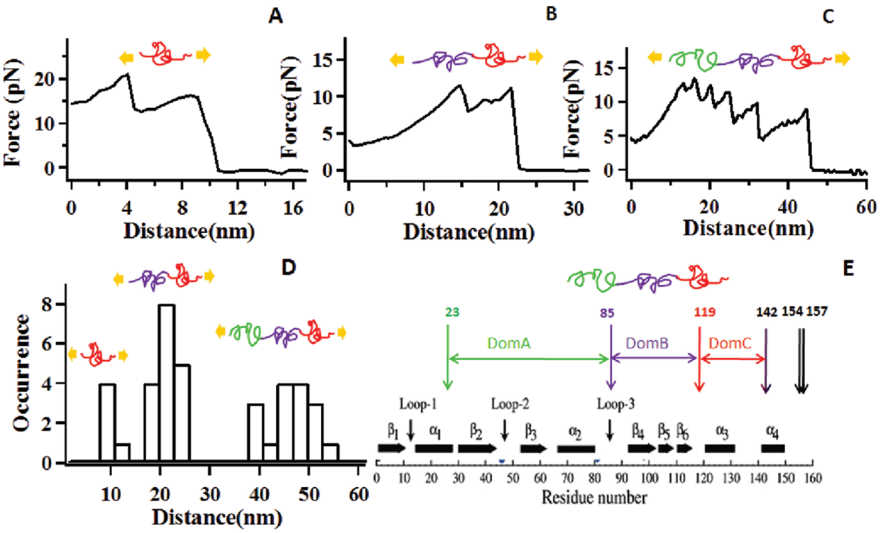

Figure 5. (A–C) Three types of single-molecule force pulling curves of HPPK, as HPPK was chemically linked to a glass coverslip at residue 142. AFM tip pulling occurs at the possible lysine residue sites 119, 85, and 23. In the insets above the force curves, three proposed domains are colored (green for DomA, purple for DomB, and red for DomC) and depicted. (A) Unfolding force curve of DomC (red), which corresponds to the rupture distance 9 nm. (B) Unfolding force curves of DomB (purple) and DomC (red), corresponding to the rupture distance 22 nm. (C) Unfolding force curve of DomA, DomB, and DomC; the rupture distance is 45 nm. (D) Histogram of the protein rupture distance distribution. The distribution of the rupture distances shows three peaks, at about 9 nm (DomC), 22 nm (DomB and DomC), and 45 nm (DomA, DomB, and Dom C). (E) Structure of the HPPK mutant (the lysine and cysteine sites are illustrated). Amino acid residue 142 was mutated to cysteine for specific site tethering of HPPK on the glass coverslip.

The results (Figure 5) show a number of significant characteristics: (1) There are multiple peaks appearing in a single domain from unfolding a single protein molecule. The multiple peaks in the single-molecule pulling force spectroscopy are primarily attributed to the traces associated with unfolding of the single segments, loops, or domains. The data are also associated with fluctuations due to the rugged landscape of protein folding with multiple local minima. For example, in Figure 5A, the force pulling curve shows two small peaks that come from the unfolding of a single protein domain DomC between residue 119 and residue 142, which suggests that our AFM-FRET nanoscopy approach is capable of probing the substructures of the protein domain from the force curves. Although, at this stage, we are not able to identify each peak with the exact fragment in the protein domains, this observation of substructures in single-molecule force spectroscopy is highly promising, which allows AFM force pulling to be a potentially powerful tool for offering insight into the details of the protein domains. (2) In the single-molecule force curve, the order of these peaks did not follow the protein structure sequence order (Figure 5E), indicating the order of the rupture did not follow the exact pattern of protein substructure sequence order in the molecule (see Supporting Information, S1). For example, the observed order of the peaks in Figure 5A (DomC) or 5B (DomB and DomC) was not the same order as in Figure 5C (DomA, DomB, and DomC). We attributed this order variance to the different overall affinity among amino acid residues in substructures to resist pulling forces, resulting in some of the substructures being easier to unfold or rupture, while others are not. We also attributed this result to the cooperative unfolding nature of the three domains; individual domains were not unfolded independently when more than one domain was stretched, as described in Figure 5B and C. (3) The force for rupturing a single protein molecule is small; the range of the force distribution is between 5 and 20 pN, as shown in the three force curves.

Our AFM-FRET nanoscopy presents a significant advancement comparing current reported techniques[29–33] in terms of conducting simultaneous single-molecule force manipulation and FRET measurement probing the corresponding conformational changes of a single targeted enzyme molecule, which is particularly powerful for studying enzyme function–conformation mechanisms and relationships between function and conformations. Nevertheless, as a typical new approach under development, there are still technical limitations that need to be addressed in further development of this combined AFM-FRET nanoscopy. For example, a major technical limitation is that the AFM tip light reflection changes the microscope photon collection efficiency depending on the tip-to-laser focus spot distance in a simultaneous AFM force manipulation and optical FRET recording experiment, the so-called AFM tip micromirror effect of changing the microscopic photon collection solid angle. In an AFM-FRET single-molecule protein pulling experiment, as the AFM tip approaches the sample surface, the micromirror effect of the AFM tip enhances the fluorescence signal collection. The enhanced signal in both

channels of donor and acceptor makes the conformational analysis from the FRET trajectory often complicated and susceptible to analysis errors. An alternative approach to remedy this complication is to use fluorescence lifetime dependent FRET measurement,[42,43] which records and analyzes the single-molecule FRET signal independently from overall intensity changes, but the temporal changes in the fluorescence decay with time. Therefore, a micromirror effect will not interfere with the single-molecule FRET measurements in recording protein conformational changes.

CONCLUSIONS

We have demonstrated a novel approach of single-molecule AFM-FRET nanoscopy that is capable of conducting simultaneous single-molecule force manipulation and FRET measurement for a targeted single protein molecule. Using this approach, we are able (1) to locate an individual Cy3−Cy5-labeled enzyme molecule in pinpoint nanoscale precision; (2) to force pull and unfold the target single enzyme molecule; and (3) to simultaneously probe the protein conformational changes by single-molecule FRET spectroscopy measurement during the AFM pulling event. Our demonstrated single-molecule AFM-FRET nanoscopy presents a novel approach of studying protein structure−function dynamics and mechanism. Using the nanoscope, we have specifically demonstrated the force pulling manipulation of a kinase enzyme and simultaneously probed the manipulated conformational changes by correlated single-molecule FRET recording, which showed multiple rupture coordinates in single-molecule enzyme force unfolding processes. AFM-FRET nanoscopy provides a new approach of analyzing the landscape of protein folding-unfolding and manipulating protein conformations to explore new properties.

EXPERIMENTAL SECTION

Sample Preparation. In preparation of the samples, we first coated the glass coverslip by covalently linking the amine group in the protein matrix with the isobutyl group of (3-aminopropyl)-trimethoxysilane and isobutyltrimethoxysilane in DMSO solution in a ratio of 1:10 000. Then we treated the coverslip surface with amine-to-amine cross-linkers (dimethyl suberimidate·2HCl, Thermo Scientific) and the HPPK kinase solutions, respectively, to cross-link an amine group in HPPK with an amine group on the coverslip surface.[44] After rinsing to remove free enzymes and residual bifunction linkers, the enzyme molecules were distributed with a low surface density of about one enzyme per μm^2 area on the coverslip surface, which is suitable and typical for single-molecule FRET fluorescence imaging measurements at the optical diffraction-limited spatial resolution. A biotin group was further attached to the tethered enzyme molecule with an amine group by immersing the sample in 10 nM EZ-link NHS-SS-Biotin, 0.1 M PBS buffer (pH = 7.4), and 0.15 M NaCl solution for 4 h.[44] After rinsing to remove unlinked biotin linkers, streptavidin was further attached to the biotin group by immersing the sample in 10 nM streptavidin solution (see Supporting Information, S3 for details).

AFM Tip Preparation. An Au-coated AFM tip (MikroMasch CSC38/Cr-Au, typical force constant K = 0.01, 0.03, 0.05 N/m) used in the experiments was first modified with a monolayer of biotin by immersing the AFM tip in 1 mM 2-aminoethanethiol solution for 4 h. The AFM tip was then further immersed in 10 nM EZ-link NHS-SS-Biotin, 0.1 M PBS buffer (pH = 7.4), and 0.15 M NaCl solution for another 4 h.[44] The interaction pair of biotin and streptavidin serves as the primary force "handle" in the AFM tip force pulling experiment (see Supporting Information, S4 for details).

Co-Axial Alignment of AFM Tip, Laser Beam Focus, and Target Molecule. The experimental setup of AFM-FRET nanoscopy is shown in detail in Figure S5 (Supporting Information, S5). The first and critical step is to line up the optical focal point and AFM tip for a typical operation of our AFM-FRET nanoscopy. First, we move the $x-y$ two-axis mechanical positioning stage to roughly align the AFM tip with the laser beam focal point by observing the light reflection pattern from the AFM tip; a symmetric light reflection pattern should be observed from the microscope objective. This indicates that the co-axial position is achieved within a few micrometers. To align the AFM tip with the laser beam center of a Gaussian distribution of the laser focus, we scan the AFM tip across the area of the laser beam that has been aligned and send one of the photon-counting signals to the AFM controller through a gated photon counter, SR400 (Stanford instruments). The image of the optical intensity was taken during an AFM tip scanning as shown in Figure S6 (Supporting Information S6). A bright spot of the optical intensity is due to the photons reflecting from the tip as the tip scans over the laser beam, because the tip can be considered as a micromirror that can reflect more photons back through the objective. Through this alignment, we are able to align the AFM tip with the center of the laser beam to a hundred nanometers.

After aligning the AFM tip with the laser beam focus in an over−under co-axial configuration, we first obtain an optical image (10 μm × 10 μm) by raster scanning the closed-loop 2D electropiezo-scanning stage with the sample over the laser focus at a scanning speed of 4 ms/pixel. Each image has a matrix density of 100 pixels × 100 pixels. We collect single-molecule fluorescence intensities of the Cy3 and Cy5 to locate single enzyme molecule positions, as shown in Figure 1B. We then move the closed-loop sample stage to move the target molecule to the center of the focal point by position control of the closed-loop $x-y$ electropiezo-scanner stage. As shown in Figure 2A, the AFM tip is exactly on top of the microscopic focal point, and it is also exactly on top of the single molecule with a few hundred nanometers' precision, which is within the optical diffraction limit. Now, the three components of AFM tip−protein−laser beam are on the same axis.

AFM Matrix Pulling (or Mapping). We conducted the AFM-FRET combined experiment in 100 mM Tris-HCl buffer and 10 mM $MgCl_2$ (pH = 8.3). To protect the FRET dyes from photobleaching, we have also added 0.8% D-glucose plus 1 mg/mL glucose oxidase, 0.04 mg/mL catalase, and about 1 mM Trolox in the mixture.[45] We utilized an approach of combined AFM 2D matrix force pulling scanning and single-molecule FRET imaging measurements. With the alignment of the AFM tip, the laser beam focus, and the target molecule in a co-axial configuration, the AFM tip and single target molecule are both in the laser focus; however, the distance between the AFM tip and the target molecule can still be in tens of nanometers away. To ensure a single-molecule AFM-FRET measurement for the same target protein molecule, we use a new approach of AFM matrix pulling (or mapping) and simultaneous single-molecule FRET measurement. The typical size of the coated AFM-tip apex is around 20−40 nm in diameter, and the HPPK enzyme molecule with streptavidin is about 5−10 nm in diameter; therefore, a 20 × 20 nm^2 area (about one pulling event area) is sufficient for each

AFM-tip pulling to ensure a direct contact with the single molecule under the laser focal point. In a typical experimental protocol, shown in Figure S7A (Supporting Information, S7), there is a 16 × 16 times pulling matrix within an area of 300 × 300 nm^2, in which an AFM-tip force pulling event occurs in every 20 nm interval. Meanwhile, the single protein molecule can be reached under such a sampling matrix of every 20 × 20 nm^2 within the laser focal point where one individual target molecule is located. Simultaneously, we record the single-molecule fluorescence intensities of the FRET pair of Cy3 and Cy5 by a two-channel photon-stamping module during the AFM matrix scanning.

Conflict of Interest: The authors declare no competing financial interest.

Acknowledgment. This work is supported by the Basic Material Science Program of the Army Research Office, and it is also supported in part by NIH NIGMS. We acknowledge stimulating discussions with Professor Honggao Yan of Michigan State University and his providing the FRET labeled HPPK protein samples.

Supporting Information Available: Detailed description of the possible amino acid residues that linked the protein molecule to the coverslip surface and to the biotin handle, detailed description of single-molecule AFM-FRET nanoscopy setup, and supporting figures are provided. This material is available free of charge *via* the Internet at http://pubs.acs.org.

REFERENCES AND NOTES

1. Boehr, D. D.; Dyson, H. J.; Wright, P. E. An NMR Perspective on Enzyme Dynamics. *Chem. Rev.* **2006**, *106*, 3055–3079.
2. Henzler-Wildman, K. A.; Lei, M.; Thai, V.; Kerns, S. J.; Karplus, M.; Kern, D. A Hierarchy of Timescales in Protein Dynamics Is Linked to Enzyme Catalysis. *Nature* **2007**, *450*, 913–916.
3. Henzler-Wildman, K. A.; Thai, V.; Lei, M.; Ott, M.; Wolf-Watz, M.; Fenn, T.; Pozharski, E.; Wilson, M. A.; Petsko, G. A.; Karplus, M.; Hubner, C. G.; Kern, D. Intrinsic Motions Along an Enzymatic Reaction Trajectory. *Nature* **2007**, *450*, 838–844.
4. Min, W.; English, B. P.; Luo, G. B.; Cherayil, B. J.; Kou, S. C.; Xie, X. S. Fluctuating Enzymes: Lessons from Single-Molecule Studies. *Acc. Chem. Res.* **2005**, *38*, 923–931.
5. Blaszczyk, J.; Li, Y.; Wu, Y.; Shi, G. B.; Ji, X. H.; Yan, H. G. Essential Roles of a Dynamic Loop in the Catalysis of 6-Hydroxymethyl-7,8-Dihydropterin Pyrophosphokinase. *Biochemistry* **2004**, *43*, 1469–1477.
6. Mittag, T.; Kay, L. E.; Forman-Kay, J. D. Protein Dynamics and Conformational Disorder in Molecular Recognition. *J. Mol. Recognit.* **2009**, *23*, 105–116.
7. Sugase, K.; Dyson, H. J.; Wright, P. E. Mechanism of Coupled Folding and Binding of an Intrinsically Disordered Protein. *Nature* **2007**, *447*, 1021–1025.
8. Wright, P. E.; Dyson, H. J. Linking Folding and Binding. *Curr. Opin. Struct. Biol.* **2009**, *19*, 31–38.
9. Boehr, D. D.; Nussinov, R.; Wright, P. E. The Role of Dynamic Conformational Ensembles in Biomolecular Recognition. *Nat. Chem. Biol.* **2009**, *5*, 789–796.
10. Guo, Z. J.; Gibson, M.; Sitha, S.; Chu, S.; Mohanty, U. Role of Large Thermal Fluctuations and Magnesium Ions in t-RNA Selectivity of the Ribosome. *Proc. Natl. Acad. Sci. U. S. A.* *108*, 3947−3951.
11. Eisenmesser, E. Z.; Bosco, D. A.; Akke, M.; Kern, D. Enzyme Dynamics during Catalysis. *Science* **2002**, *295*, 1520–1523.
12. Tan, X.; Nalbant, P.; Toutchkine, A.; Hu, D. H.; Vorpagel, E. R.; Hahn, K. M.; Lu, H. P. Single-Molecule Study of Protein-Protein Interaction Dynamics in a Cell Signaling System. *J. Phys. Chem. B* **2004**, *108*, 737–744.
13. Tan, X.; Hu, D. H.; Squier, T. C.; Lu, H. P. Probing Nanosecond Protein Motions of Calmodulin by Single-Molecule Fluorescence Anisotropy. *Appl. Phys. Lett.* **2004**, *85*, 2420–2422.
14. Zhang, Q.; Stelzer, A. C.; Fisher, C. K.; Al-Hashimi, H. M. Visualizing Spatially Correlated Dynamics That Directs RNA Conformational Transitions. *Nature* **2007**, *450*, 1263–1267.
15. Mittermaier, A. K.; Kay, L. E. Observing Biological Dynamics at Atomic Resolution Using NMR. *Trends Biochem. Sci.* **2009**, *34*, 601–611.
16. Pan, R.; Zhang, X. J.; Zhang, Z. J.; Zhou, Y.; Tian, W. X.; He, R. Q. Substrate-Induced Changes in Protease Active Site Conformation Impact on Subsequent Reactions with Substrates. *J. Biol. Chem.* **2010**, *285*, 22948–22954.
17. Lu, H. P.; Iakoucheva, L. M.; Ackerman, E. J. Single-Molecule Conformational Dynamics of Fluctuating Noncovalent DNA-Protein Interactions in DNA Damage Recognition. *J. Am. Chem. Soc.* **2001**, *123*, 9184–9185.
18. Harms, G.; Orr, G.; Lu, H. P. Probing Ion Channel Conformational Dynamics Using Simultaneous Single-Molecule Ultrafast Spectroscopy and Patch-Clamp Electric Recording. *Appl. Phys. Lett.* **2004**, *84*, 1792–1794.
19. Harms, G. S.; Orr, G.; Montal, M.; Thrall, B. D.; Colson, S. D.; Lu, H. P. Probing Conformational Changes of Gramicidin Ion Channels by Single-Molecule Patch-Clamp Fluorescence Microscopy. *Biophys. J.* **2003**, *85*, 1826–1838.
20. Lomholt, M. A.; Urbakh, M.; Metzler, R.; Klafter, J. Manipulating Single Enzymes by an External Harmonic Force. *Phys. Rev. Lett.* **2007**, *98*, 168302.
21. Astumian, R. D.; Robertson, B. Imposed Oscillations of Kinetic Barriers Can Cause an Enzyme to Drive a Chemical-Reaction Away from Equilibrium. *J. Am. Chem. Soc.* **1993**, *115*, 11063–11068.
22. Wiita, A. P.; Ainavarapu, S. R. K.; Huang, H. H.; Fernandez, J. M. Force-Dependent Chemical Kinetics of Disulfide Bond Reduction Observed with Single-Molecule Techniques. *Proc. Natl. Acad. Sci. U. S. A.* **2006**, *103*, 7222–7227.
23. Wiita, A. P.; Perez-Jimenez, R.; Walther, K. A.; Grater, F.; Berne, B. J.; Holmgren, A.; Sanchez-Ruiz, J. M.; Fernandez, J. M. Probing the Chemistry of Thioredoxin Catalysis with Force. *Nature* **2007**, *450*, 124–127.
24. Lu, H. P. Single-Molecule Spectroscopy Studies of Conformational Change Dynamics in Enzymatic Reactions. *Curr. Pharm. Biotechnol.* **2004**, *5*, 261–269.
25. Lu, H. P.; Xun, L. Y.; Xie, X. S. Single-Molecule Enzymatic Dynamics. *Science* **1998**, *282*, 1877–1882.
26. Lu, H. P. Probing Single-Molecule Protein Conformational Dynamics. *Acc. Chem. Res.* **2005**, *38*, 557–565.
27. Junker, J. P.; Rief, M. Single-Molecule Force Spectroscopy Distinguishes Target Binding Modes of Calmodulin. *Proc. Natl. Acad. Sci. U. S. A.* **2009**, *106*, 14361–14366.
28. Junker, J. P.; Ziegler, F.; Rief, M. Ligand-Dependent Equilibrium Fluctuations of Single Calmodulin Molecules. *Science* **2009**, *323*, 633–637.
29. Gumpp, H.; Puchner, E. M.; Zimmermann, J. L.; Gerland, U.; Gaub, H. E.; Blank, K. Triggering Enzymatic Activity with Force. *Nano Lett.* **2009**, *9*, 3290–3295.
30. Sarkar, A.; Robertson, R. B.; Fernandez, J. M. Simultaneous Atomic Force Microscope and Fluorescence Measurements of Protein Unfolding Using a Calibrated Evanescent Wave. *Proc. Natl. Acad. Sci. U. S. A.* **2004**, *101*, 12882–12886.
31. Kodama, T.; Ohtani, H.; Arakawa, H.; Ikai, A. Mechanical Perturbation-Induced Fluorescence Change of Green Fluorescent Protein. *Appl. Phys. Lett.* **2005**, *86*, 043901.
32. Gaiduk, A.; Kuhnemuth, R.; Felekyan, S.; Antonik, M.; Becker, W.; Kudryavtsev, V.; Sandhagen, C.; Seidel, C. A. M. Fluorescence Detection with High Time Resolution: From Optical Microscopy to Simultaneous Force and Fluorescence Spectroscopy. *Microsc. Res. Tech.* **2007**, *70*, 433–441.
33. Kellermayer, M. S. Z.; Karsai, A.; Kengyel, A.; Nagy, A.; Bianco, P.; Huber, T.; Kulcsar, A.; Niedetzky, C.; Proksch, R.; Grama, L. Spatially and Temporally Synchronized Atomic Force and Total Internal Reflection Fluorescence Microscopy for Imaging and Manipulating Cells and Biomolecules. *Biophys. J.* **2006**, *91*, 2665–2677.
34. Li, Y.; Gong, Y. C.; Shi, G. B.; Blaszczyk, J.; Ji, X. H.; Yan, H. G. Chemical Transformation Is Not Rate-Limiting in the Reaction Catalyzed by Escherichia Coli 6-Hydroxymethyl-7,8-Dihydropterin Pyrophosphokinase. *Biochemistry* **2002**, *41*, 8777–8783.
35. *We Received the FRET Donor−Acceptor Dye-Labeled HPPK Samples from Professor Honggao Yan of Michigan State University.*

36. Ha, T. J.; Ting, A. Y.; Liang, J.; Caldwell, W. B.; Deniz, A. A.; Chemla, D. S.; Schultz, P. G.; Weiss, S. Single-Molecule Fluorescence Spectroscopy of Enzyme Conformational Dynamics and Cleavage Mechanism. *Proc. Natl. Acad. Sci. U. S. A.* **1999**, *96*, 893–898.
37. Roy, R.; Hohng, S.; Ha, T. A Practical Guide to Single-Molecule FRET. *Nat. Methods* **2008**, *5*, 507–516.
38. Hinterdorfer, P.; Oijen, A. v. *Handbook of Single-Molecule Biophysics*; Springer: Berlin, 2009.
39. Rief, M.; Gautel, M.; Oesterhelt, F.; Fernandez, J. M.; Gaub, H. E. Reversible Unfolding of Individual Titin Immunoglobulin Domains by AFM. *Science* **1997**, *276*, 1109–1112.
40. Rief, M.; Fernandez, J. M.; Gaub, H. E. Elastically Coupled Two-Level Systems as a Model for Biopolymer Extensibility. *Phys. Rev. Lett.* **1998**, *81*, 4764–4767.
41. Cecconi, C.; Shank, E. A.; Bustamante, C.; Marqusee, S. Direct Observation of the Three-State Folding of a Single Protein Molecule. *Science* **2005**, *309*, 2057–2060.
42. Hu, D. H.; Micic, M.; Klymyshyn, N.; Suh, Y. D.; Lu, H. P. Correlated Topographic and Spectroscopic Imaging Beyond Diffraction Limit by Atomic Force Microscopy Metallic Tip-Enhanced Near-Field Fluorescence Lifetime Microscopy. *Rev. Sci. Instrum.* **2003**, *74*, 3347–3355.
43. Ratchford, D.; Shafiei, F.; Kim, S.; Gray, S. K.; Li, X. Q. Manipulating Coupling between a Single Semiconductor Quantum Dot and Single Gold Nanoparticle. *Nano Lett.* **2011**, *11*, 1049–1054.
44. Hermanson, G. T. *Bioconjugate Techniques*, 2nd ed.; Academic Press: New York, 2008.
45. Selvin, P. R.; Ha, T. *Single-Molecule Techniques: A Laboratory Manual*; Cold Spring Harbor Laboratory Press, 2008.